

## ENDOR Evidence of Electron–H<sub>2</sub> Interaction in a Fulleride Embedding H<sub>2</sub>

Alfonso Zoleo,<sup>†</sup> Ronald G. Lawler,<sup>‡</sup> Xuegong Lei,<sup>§</sup> Yongjun Li,<sup>§</sup> Yasujiro Murata,<sup>⊥</sup> Koichi Komatsu,<sup>||</sup> Marilena Di Valentin,<sup>†</sup> Marco Ruzzi,<sup>†</sup> and Nicholas J. Turro<sup>\*,§</sup>

<sup>†</sup>Department of Chemistry, University of Padova, via Marzolo 1, I-35131 Padova, Italy

<sup>‡</sup>Brown University, Providence, Rhode Island 02912-9108, United States

<sup>§</sup>Department of Chemistry, Columbia University, New York, New York 10027, United States

<sup>⊥</sup>Institute for Chemical Research, Kyoto University, Uji, Kyoto 611-0011, Japan

<sup>||</sup>Department of Environmental and Biological Chemistry, Fukui University of Technology, Gakuen, Fukui 910-8505, Japan

### S Supporting Information

**ABSTRACT:** An endofulleropyrrolidine, with H<sub>2</sub> as a guest, has been reduced to a paramagnetic endofulleride radical anion. The magnetic interaction between the electron delocalized on the fullerene cage and the guest H<sub>2</sub> has been probed by pulsed ENDOR. The experimental hyperfine couplings between the electron and the H<sub>2</sub> guest were measured, and their values agree very well with DFT calculations. This agreement provides clear evidence of magnetic communication between the electron density of the fullerene host cage and H<sub>2</sub> guest. The *ortho*-H<sub>2</sub>/*para*-H<sub>2</sub> interconversion is revealed by temperature-dependent ENDOR measurements at low temperature. The conversion of the paramagnetic *ortho*-H<sub>2</sub> to the diamagnetic *para*-H<sub>2</sub> causes the ENDOR signal to decrease as the temperature is lowered due to the spin catalysis by the paramagnetic fullerene cage of the radical anion fulleride.

The recent availability of endofullerenes containing encapsulated H<sub>2</sub> and D<sub>2</sub> molecules (H<sub>2</sub>@C<sub>60</sub> and D<sub>2</sub>@C<sub>60</sub>)<sup>1</sup> has provided an opportunity to investigate the effect of the endo H<sub>2</sub> molecule on the properties of the C<sub>60</sub> cage (effect on <sup>1</sup>O<sub>2</sub> quenching rate)<sup>2</sup> as well as the effect of the cage on the properties of the incarcerated H<sub>2</sub> (nuclear spin–lattice relaxation time,<sup>3</sup> nuclear relaxation by external paramagnets,<sup>4</sup> *ortho/para* conversion rate<sup>5</sup>). The coupling between translational and rotational states of the endo guest H<sub>2</sub> has been detected experimentally by infrared (IR)<sup>6a</sup> and inelastic neutron scattering (INS)<sup>6b</sup> experiments on H<sub>2</sub>@C<sub>60</sub>. Excellent agreement with theory<sup>7</sup> provides a striking confirmation of the influence of the incarceration of H<sub>2</sub> into a fullerene cage on the rotational and translational dynamics of the caged H<sub>2</sub>.

In the cases studied to date, although there are detectable mutual effects on the properties of both the host fullerene cage and the guest H<sub>2</sub>, there has not been a report of direct evidence for coupling between the endo H<sub>2</sub> and the nuclei or electrons associated with the cage itself. For example, the <sup>13</sup>C T<sub>1</sub> of the carbon cage is not affected by the presence of the endo H<sub>2</sub>.<sup>8</sup> Similarly, the interactions of incarcerated H<sub>2</sub> and D<sub>2</sub> with the excited triplet of fullerene <sup>3</sup>C<sub>60</sub> were found to be too weak to be measured by either triplet lifetime measurements (triplet–

triplet absorption) or time-resolved EPR spectroscopy.<sup>2</sup> The dipolar interaction between H<sub>2</sub> and the unpaired electron in a derivative of H<sub>2</sub>@C<sub>60</sub> containing an attached nitroxide group has been detected only indirectly through the effect on the proton relaxation time of the endo H<sub>2</sub>.<sup>9</sup>

In contrast to negative or, at best, indirect evidence of the above types for communication between the endo H<sub>2</sub> with the surrounding fullerene cage or molecular species external to the fullerene, we report here the direct observation by electron nuclear double resonance (ENDOR) of hyperfine interaction (hfi) between the surface-delocalized unpaired electron in the radical anion of a modified fullerene and the protons of an endo H<sub>2</sub> molecule.<sup>10</sup>

In addition to the interest inherent in the ENDOR results reported here, the interaction of the cage electron with H<sub>2</sub> has important implications for the *ortho/para* nuclear spin conversion catalysis of H<sub>2</sub> incarcerated in C<sub>60</sub>. In a previous report<sup>11</sup> we established that the H<sub>2</sub> molecule inside C<sub>60</sub> exists as a mixture of *ortho*-H<sub>2</sub> and *para*-H<sub>2</sub> and that the forward conversion of *ortho*-H<sub>2</sub> to *para*-H<sub>2</sub> can be catalyzed by external paramagnetic species; furthermore, the back conversion (from *para*-H<sub>2</sub> to *ortho*-H<sub>2</sub>) is much slower for H<sub>2</sub> inside the cage than for free H<sub>2</sub> in the same solution. In that work *para*-enrichment of the endo H<sub>2</sub> was obtained by dispersing H<sub>2</sub>@C<sub>60</sub> on the external surface of a zeolite, employing liquid oxygen at 77 K as a physically removable paramagnetic spin catalyst.

The results presented in this Communication may be considered a preliminary step toward the setting up of a new experimental light-induced approach for catalyzing the *ortho*-H<sub>2</sub>/*para*-H<sub>2</sub> conversion inside a fullerene cage using reversible formation of the radical ion as the catalyst. It was reported that, under continuous light irradiation, an electron-donor linked to C<sub>60</sub> derivatives undergoes fast, reversible photoinduced electron transfer to generate fullerene radical monoanions with high efficiency.<sup>12</sup> Furthermore, in these donor–fullerene compounds, charge recombination (back electron transfer) is very efficient, the fullerene monoanion transient absorption signal decaying typically within a few hundred microseconds or less. Such systems allow the *ortho/para* conversion of H<sub>2</sub> inside the

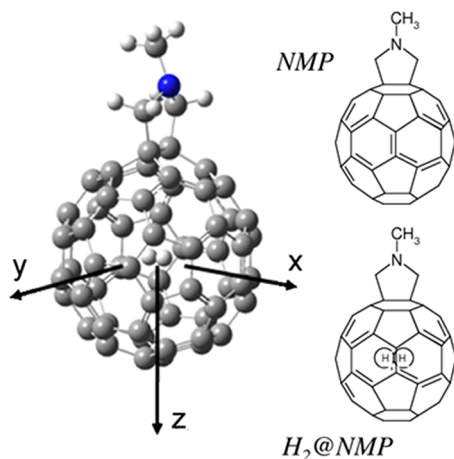
Received: January 5, 2012

Published: July 19, 2012

cage to be activated by illumination at low temperature and subsequently, when the enrichment has been obtained, to deactivate the back conversion, even after the temperature has been raised, by turning off the light (optical switch).

In this work  $\text{H}_2\text{@NMP}$  and, for comparison, NMP (the same fulleropyrrolidine lacking  $\text{H}_2$ , Chart 1) were reduced to radical

**Chart 1.** (Left)  $\text{H}_2\text{@NMP}$  Structure Showing the  $x$ ,  $y$ , and  $z$  Axes and (Right) Line Drawings of NMP and  $\text{H}_2\text{@NMP}$



monoanions in 2-MeTHF, according to the procedure reported previously.<sup>13</sup> CW-EPR spectra of both fullerides were acquired in the temperature range from 290 to 80 K, carefully adjusting the radical concentration in order to minimize the line width of the EPR signal. The  $\text{H}_2\text{@NMP}$  and NMP monoanion spectra appear very similar in this temperature range and exhibit the well-known features attributable to the hyperfine coupling with the pyrrolidinic nitrogen (three lines in the ratio 1:1:1) and smaller lines on the wings due to  $^{13}\text{C}$  couplings.<sup>14</sup> No further splitting attributable to coupling with *ortho*- $\text{H}_2$  is observable in the  $\text{H}_2\text{@NMP}$  monoanion spectra, even in the liquid solution at 160 K, where the line width is the narrowest, although there may be additional broadening of the  $\text{H}_2\text{@NMP}$  peaks. Experimental and simulated CW-EPR spectra of NMP and  $\text{H}_2\text{@NMP}$  monoanions are shown in the Supporting Information, Figure S1, with a detailed discussion.

Superhyperfine couplings that are unresolved by ordinary EPR may often be detected by ENDOR or ESEEM. Pulsed ENDOR techniques are now preferred to the CW-ENDOR approach, due to their superior time stability and relative independence of relaxation times, provided that relaxation times are long enough.<sup>15</sup> The main limitation of pulsed ENDOR is the requirement of a strong electron spin echo, which in NMP monoanion is experimentally observed only below 100 K in frozen 2-MeTHF. Above this temperature, electron spin relaxation times are too fast, and the electron spin echo decays within the instrumental “dead time”,<sup>16</sup> i.e., within the time after the last pulse during which the detector is not able to record the signal. Pulsed Davies ENDOR spectra<sup>17</sup> of NMP and  $\text{H}_2\text{@NMP}$  monoanions were acquired in the temperature range from 100 to 50 K, and are shown in Figure 1. The radio frequency was swept from 13.5 to 16 MHz in order to select the proton ENDOR signals.

The dominant feature in the  $^1\text{H}$  ENDOR spectra of both radicals is due to the overlap of unresolved ENDOR signals from the pyrrolidinic protons and a possible signal from dipolar

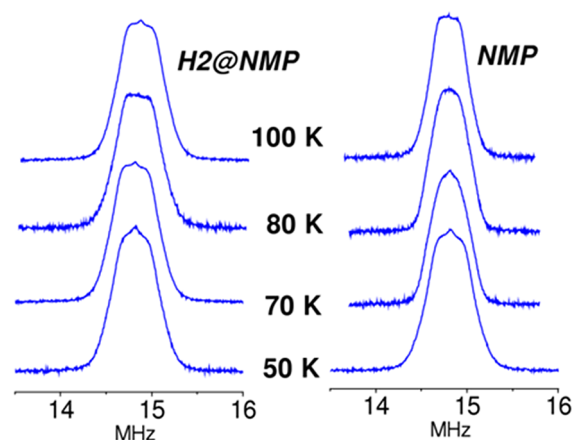


**Figure 1.** Pulsed ENDOR spectra (Davies-type ENDOR) of NMP and  $\text{H}_2\text{@NMP}$  monoanions in frozen solutions of 2-MeTHF at different temperatures.

coupling to solvent protons (free proton line).<sup>18</sup> For  $\text{H}_2\text{@NMP}$  monoanion, we expect also hyperfine couplings with the endo hydrogen molecule, only if the  $\text{H}_2$  is in the *ortho* state ( $I = 1$ ), since the *para* state ( $I = 0$ ) is diamagnetic and undetectable by NMR or ENDOR. In order to estimate the magnitude of hyperfine contribution, we performed DFT calculations on  $\text{H}_2\text{@NMP}$  monoanion. We optimized the structure of neutral NMP at level PM3, and located the  $\text{H}_2$  molecule in the center of the buckyball. We took into account three orthogonal orientations of the  $\text{H}_2$  molecule inside the fulleropyrrolidine (Chart 1): along the  $x$ ,  $y$ , and  $z$  axes. We performed DFT calculations on the three configurations by using the basis set 6-31G(d,p) and the hybrid functional B3LYP<sup>19</sup> with the software package Gaussian 09.<sup>20</sup> Solvent was also taken into account (PCM model; solvent, THF).<sup>21</sup> We are aware that this is a very rough approach, and more refined calculations will be necessary in the future.

Results of hyperfine calculations for all the protons are reported in Table 1: the isotropic hyperfine couplings  $A_{\text{iso}}$ , the principal components of the dipolar hyperfine tensor  $T_1$ ,  $T_2$ , and  $T_3$ , and the pseudoaxial  $T_{\text{dip}}$ , which is calculated as  $1/2 T_3$ . The hyperfine couplings for  $\text{H}_2$  have been calculated in the  $x$ ,  $y$ , and  $z$  directions and averaged over the three orientations, which is roughly the value one expects to see experimentally on the EPR time scale, as  $\text{H}_2$  tumbles very fast inside the buckyball. Also the methyl group is rotating very rapidly on the EPR time scale, and we suppose that the methyl protons are magnetically equivalent, assuming an averaged hyperfine tensor. Calculations on a nonplanar structure indicate that the four protons attached to the pyrrolidinic ring would all have similar hyperfine parameters. For simplicity, therefore, we report the averaged values of the parameters in Table 1.

According to the calculations, the hyperfine coupling with the  $\text{H}_2$  inside is substantially smaller than the CW-EPR line width (ca. 30 kHz) and of the same order as the methyl proton hyperfine couplings. The hyperfine couplings are so small that it does not come as a surprise that neither the CW-EPR (Figure S1) nor ENDOR spectra (Figure 1) are well resolved. However, a careful comparison of the ENDOR spectra of NMP and  $\text{H}_2\text{@NMP}$  monoanions at all but the lowest temperature, 50 K, shows a clear difference in the ENDOR profiles for the two species, the ENDOR peak of  $\text{H}_2\text{@NMP}$  monoanion being significantly “flattened” and broadened. A

Table 1. Calculated (DFT-B3LYP-6-31G(d,p)) and Experimental<sup>a</sup> H Hyperfine Couplings (in MHz) for H<sub>2</sub>@NMP Monoanion

|                                   | $A_{\text{iso}}$ | $T_1$ | $T_2$ | $T_3$ | $T_{\text{dip}}$   |
|-----------------------------------|------------------|-------|-------|-------|--------------------|
| pyrrolidine <sup>b</sup>          | -0.17            | -0.26 | -0.12 | 0.38  | 0.19 <sup>f</sup>  |
| methyl <sup>b</sup>               | -0.035           | -0.12 | -0.10 | 0.22  | 0.11 <sup>f</sup>  |
| H <sub>2</sub> (x) <sup>c</sup>   | -0.12            | 0.49  | 0.25  | -0.74 | -0.37 <sup>f</sup> |
| H <sub>2</sub> (y) <sup>c</sup>   | -0.12            | 0.49  | 0.23  | -0.72 | -0.36 <sup>f</sup> |
| H <sub>2</sub> (z) <sup>c</sup>   | -0.12            | 0.49  | 0.27  | -0.76 | -0.38 <sup>f</sup> |
| H <sub>2</sub> (av) <sup>d</sup>  | -0.12            | 0.49  | 0.25  | -0.74 | -0.37 <sup>f</sup> |
| H <sub>2</sub> (exp) <sup>e</sup> | -0.10 ± 0.02     |       |       |       | -0.45 ± 0.03       |

<sup>a</sup>From fitting of observed and simulated spectra (Figure 2). <sup>b</sup>Averaged values of the calculated isotropic hyperfine coupling and anisotropic main components for pyrrolidinic and ring protons. <sup>c</sup>Calculated isotropic hyperfine coupling and anisotropic main components for the H<sub>2</sub> molecule located along x, y, z. <sup>d</sup>Averaged values of the calculated hyperfine couplings reported for H<sub>2</sub>(x), H<sub>2</sub>(y), and H<sub>2</sub>(z). <sup>e</sup>H<sub>2</sub> hyperfine parameters from simulation of the experimental ENDOR difference spectrum at 70 K (Figure 2). <sup>f</sup>Considering  $T_{\text{dip}} = 1/2 T_3$ .

difference spectrum has been computed for the spectra recorded at each temperature, subtracting the NMP<sup>-</sup> ENDOR spectrum from the H<sub>2</sub>@NMP<sup>-</sup> ENDOR spectrum. The difference removes all the lines due to hyperfine couplings with identical nuclei present in both the samples. For calculating the ENDOR difference spectrum we used the formula  $Z = Y - kX$ , where Z is the difference spectrum, Y is the H<sub>2</sub>@NMP<sup>-</sup> ENDOR spectrum, X is the NMP<sup>-</sup> ENDOR spectrum, and k is a scale-factor that takes into account the slightly different amount of the two samples, instrumental differences due to sample position in the probehead, and slightly different EPR tubes. The scale-factor k was chosen in order to have the difference spectrum well resolved and fully positive. Note that the value of k does not affect the line position in the difference spectrum Z. The difference spectrum Z, computed according to the previous formula, for the spectra X and Y recorded at 70 K and with  $k = 0.8$  is shown in Figure 2

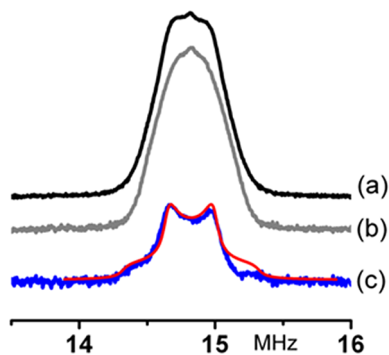


Figure 2. ENDOR spectra recorded at 70 K of H<sub>2</sub>@NMP (a) and NMP (b) monoanions; (c) difference spectrum (blue line) between (a) and (b) with its simulation (red line).

(spectrum c, blue line). The difference spectra calculated at each temperature in the range 50–100 K (keeping  $k = 0.8$  constant) are shown in the Supporting Information, Figure S2.

The spectral profile of Z shown in Figure 2c is typical for the anisotropic coupling with one (or more equivalent) proton(s), characterized by an axial hyperfine tensor. Since the ENDOR difference removes all the lines that are due to hyperfine couplings with identical nuclei present in both samples, such a difference can be attributed to the hyperfine coupling with the nuclei of H<sub>2</sub> in H<sub>2</sub>@NMP<sup>-</sup>.

In order to verify this assignment, simulation of the difference spectrum Z at 70 K was carried out: a very good simulation (Figure 2, spectrum c, red line) was obtained with the hyperfine isotropic and anisotropic constants reported in

the last row of Table 1. The simulation was performed with a homemade program written for the MatLab platform, version 7.0.1. The nuclear spin Hamiltonian was taken in the high-field approximation (with only secular terms  $I_z S_z$  and  $S_z I_z$ ), and an axial hyperfine tensor was used. In Table 1 also the pseudoaxial tensor component  $T_{\text{dip}}$  has been reported for all the calculated proton hyperfine couplings, in order to allow the comparison with the isotropic and anisotropic constants obtained from the simulation (last row of Table 1). Note that the hyperfine isotropic and anisotropic constants employed in the simulation are in very good agreement with the DFT-calculated anisotropic and isotropic hyperfine couplings for the H<sub>2</sub> molecule (second-to-last row of Table 1), both in sign and in magnitude, and markedly different from the DFT-calculated hfi values for pyrrolidinic and methyl protons (first and second rows of Table 1).

The attribution of the difference spectrum Z to the interaction with the encapsulated *ortho*-H<sub>2</sub> is supported also by the temperature dependence of both the intensity and line shape of Z. At higher temperatures (90–100 K, see Figure S2) the difference spectrum broadens to coalescence to a single peak. In this case the ENDOR peak is too broad to resolve the 100 kHz doublet expected for a rapidly tumbling *ortho*-H<sub>2</sub> molecule. Lowering the temperature, the odd electron on the fullerene cage catalyzes the *ortho/para* conversion. Since the diamagnetic nuclear *para* spin isomer is the lower energy state, the *ortho/para* conversion results in a progressive reduction of the *ortho*-H<sub>2</sub> ENDOR signal, which becomes undetectable below 50 K. Note that each ENDOR spectrum was acquired after the ENDOR signals appeared approximately steady (about 1 h after the temperature was set up in the cryostat). This means that the time of interconversion of the *ortho*-H<sub>2</sub>/*para*-H<sub>2</sub> in the fulleride is enormously faster (order of minutes) than that of the parent neutral, diamagnetic species, which would be expected to have a conversion rate similar to that of H<sub>2</sub>@C<sub>60</sub> (weeks).<sup>11</sup>

In conclusion, despite the approximate approach used for the calculations, the excellent agreement we obtained between experimental and calculated values supports the assignments of the observed lines in the ENDOR difference spectrum. On the basis of this assignment, the weak magnetic interaction between the electron on the buckyball and the inner H<sub>2</sub> has been estimated here for the first time, proving definitively the existence of a “communication” between the electron density on the fulleride buckyball and the incarcerated H<sub>2</sub> molecule.<sup>22</sup> Moreover, in accordance with the presence of this magnetic interaction, evidence of a very efficient spin catalysis due to the free electron of the fulleride is given, the time of the *ortho*-H<sub>2</sub>/



*para*-H<sub>2</sub> conversion being not longer than 1 h. ENDOR (in addition to NMR and Raman spectroscopies) is then potentially able to follow at several temperatures the *ortho/para* conversion in suitable paramagnetic systems.

## ■ ASSOCIATED CONTENT

### ● Supporting Information

Details about the CW-EPR and ENDOR instrumental setup and measurements, CW-EPR spectra and simulations, supplementary experimental ENDOR results (difference spectra of both H<sub>2</sub>@NMP and NMP monoanions at different temperatures), and control experiments (ENDOR spectra recorded at different microwave and RF pulse lengths). This material is available free of charge via the Internet at <http://pubs.acs.org>.

## ■ AUTHOR INFORMATION

### Corresponding Author

njt3@columbia.edu

### Notes

The authors declare no competing financial interest.

## ■ ACKNOWLEDGMENTS

The authors at Columbia thank the National Science Foundation for generous support of this research through grants CHE 11 11398 and CHE 07 17518. We are deeply thankful to Prof. Marina Brustolon and Prof. Donatella Carbonera (Dept. of Chemical Sciences, Padova University) for their technical support to this research. We acknowledge Dr. Lorenzo Franco (Dept. of Chemical Sciences, Padova University) and Dr. Elena Sartori for the helpful discussions and comments. We are grateful to Mr. Alberto Collauto for the contribution on the DFT calculations. We thank Mrs. Manuela Zangirolami and Mrs. Sabrina Mattiolo (Dept. of Chemical Sciences, Padova University) for their technical contribution on the fullerene reductions.

## ■ REFERENCES

- (1) Komatsu, K.; Murata, M.; Murata, Y. *Science* **2005**, *307*, 238.
- (2) López-Gejo, J.; Martí, A. A.; Ruzzi, M.; Jockusch, S.; Komatsu, K.; Tanabe, F.; Murata, Y.; Turro, N. J. *J. Am. Chem. Soc.* **2007**, *129*, 14554.
- (3) Sartori, E.; Ruzzi, M.; Turro, N. J.; Decatur, J. D.; Doetschman, D. C.; Lawler, R. G.; Buchachenko, A. L.; Murata, Y.; Komatsu, K. *J. Am. Chem. Soc.* **2006**, *128*, 14752.
- (4) Sartori, E.; Ruzzi, M.; Turro, N. J.; Komatsu, K.; Murata, Y.; Lawler, R. G.; Buchachenko, A. L. *J. Am. Chem. Soc.* **2008**, *130*, 2221.
- (5) Sartori, E.; Ruzzi, M.; Lawler, R. G.; Turro, N. J. *J. Am. Chem. Soc.* **2008**, *130*, 12752.
- (6) (a) Mamone, S.; Ge, Min; Hüvonen, D.; Nagel, U.; Danquigny, A.; Cuda, F.; Grossel, M. C.; Murata, Y.; Komatsu, K.; Levitt, M. H.; Rööm, T.; Carravetta, M. *J. Chem. Phys.* **2009**, *130*, 081103. (b) Horsewill, A. J.; Rols, S.; Johnson, M. R.; Murata, Y.; Murata, M.; Komatsu, K.; Carravetta, M.; Mamone, S.; Levitt, M. H.; Chen, J. Y.-C.; Johnson, J. A.; Lei, X.; Turro, N. J. *Phys. Rev. B* **2010**, *82*, 081410(R).
- (7) (a) Xu, M.; Sebastianelli, F.; Bačić, Z.; Lawler, R.; Turro, N. J. *J. Chem. Phys.* **2008**, *128*, 011101. (b) Xu, M.; Sebastianelli, F.; Bačić, Z.; Lawler, R.; Turro, N. J. *J. Chem. Phys.* **2008**, *129*, 064313. (c) Xu, M.; Sebastianelli, F.; Gibbons, B. R.; Bačić, Z.; Lawler, R.; Turro, N. J. *J. Chem. Phys.* **2009**, *130*, 224306.
- (8) SUFIR (SUper Fast Inversion Recovery) measurements in deoxygenated 1,2-dichlorobenzene-*d*<sub>4</sub> at 290 K showed that <sup>13</sup>C T<sub>1</sub> for C<sub>60</sub> and H<sub>2</sub>@C<sub>60</sub> were 91.0 and 90.4 s, respectively, with an estimated error of ca. ±5% (Dr. Elena Sartori, unpublished results).
- (9) (a) Li, Y.; Lei, X.; Lawler, R. G.; Murata, Y.; Komatsu, K.; Turro, N. J. *J. Phys. Chem. Lett.* **2010**, *1*, 2135. (b) Li, Y.; Lei, X.; Li, X.; Lawler, R. G.; Murata, Y.; Komatsu, K.; Turro, N. J. *Chem. Commun.* **2011**, *47*, 12527.
- (10) This report does not represent the first time that ENDOR has been used to detect the interaction between a species embedded in fullerene and the outer world. In previous work, a Q-band CW-ENDOR study of a fullerene C<sub>82</sub> possessing an embedded La atom was reported. The interaction between the spin density of the La@C<sub>82</sub> system and the matrix protons was detected: (a) Koltover, V. K. *J. Mol. Liq.* **2005**, *120*, 151. (b) Koltover, V. K.; Bubnov, V. P.; Estrin, Y. I.; Lodygina, V. P.; Davydov, R. M.; Subramoni, M.; Manoharan, P. T. *Phys. Chem. Chem. Phys.* **2003**, *5*, 2774. However, the latter case is special, since the guest@host system involves a large and special lanthanide earth atom inside an uncommon fullerene, C<sub>82</sub>. In contrast, we report by ENDOR the detection of a magnetic interaction involving a small but fundamental and well-studied molecule, H<sub>2</sub>, embedded in a very common fullerene C<sub>60</sub> derivative (NMP).
- (11) Turro, N. J.; Martí, A. A.; Chen, J. Y. C.; Jockusch, S.; Lawler, R. G.; Ruzzi, M.; Sartori, E.; Chuang, S. C.; Komatsu, K.; Murata, Y. *J. Am. Chem. Soc.* **2008**, *130*, 10506.
- (12) (a) Imahori, H.; Sakata, Y. *Eur. J. Org. Chem.* **1999**, 2445. (b) Martín, N.; Sánchez, L.; Illescas, B.; Pérez, I. *Chem. Rev.* **1998**, *98*, 2527.
- (13) Zoleo, A.; Maniero, A. L.; Bellinazzi, M.; Prato, M.; Da Ros, T.; Brunel, L. C.; Brustolon, M. *J. Magn. Reson.* **2002**, *159*, 226.
- (14) (a) Zoleo, A.; Maniero, A. L.; Prato, M.; Severin, M. G.; Brunel, L. C.; Kordatos, K.; Brustolon, M. *J. Phys. Chem. A* **2000**, *104*, 9853. (b) Brustolon, M.; Zoleo, A.; Agostini, G.; Maggini, M. *J. Phys. Chem. A* **1998**, *102*, 6331.
- (15) (a) Gemperle, C.; Schweiger, A. *Chem. Rev.* **1991**, *91*, 1481. (b) Schweiger, A.; Jeschke, G.; *Principle of Pulse Electron Paramagnetic Resonance*; Oxford University Press: Oxford, 2001.
- (16) Instrumental dead time in our spectrometer is estimated below 200 ns.
- (17) Davies, E. R. *Phys. Lett. A* **1974**, *47A*, 1.
- (18) Both features could be minimized relative to the H<sub>2</sub> signal by the use of perdeuterated solvent and replacement of the methyl and ring protons with deuterium. Although both methodologies will surely be employed for refined ENDOR studies of these and other endofullerenes, the expense and synthetic effort required was not deemed necessary for this initial investigation.
- (19) (a) Lee, C.; Yang, W.; Parr, R. G. *Phys. Rev.* **1988**, *B37*, 785. (b) Becke, A. D. *J. Chem. Phys.* **1993**, *98*, 56.
- (20) Frisch, M. J.; et al. *Gaussian 09*, Revision B.01; Gaussian, Inc.: Wallingford, CT, 2010.
- (21) (a) Miertus, S.; Scrocco, E.; Tomasi, J. *J. Chem. Phys.* **1981**, *55*, 117. (b) Cammi, R.; Tomasi, J. *J. Comput. Chem.* **1995**, *16*, 1449.
- (22) In a recent study [see ref 9b, electronic supporting information] of a H<sub>2</sub>@C<sub>60</sub> nitroxide analogous to NMP, in which the N-CH<sub>3</sub> group was replaced by N-O• and the pyrrolidine protons were replaced by methyl groups, we have compared the relaxation times, positions, and widths of the endo H<sub>2</sub> peaks for the nitroxide with those for the corresponding, diamagnetic hydroxylamine. It is concluded that any hyperfine coupling between the external unpaired electron and the endohedral protons is less than 1 mG (ca. 0.003 MHz), i.e., less than 1% of the value reported here for the unpaired electron confined to the surface of the fullerene.